

# Exclusive Hard Diffraction at HERA (DVCS and Vector Mesons)

*Pierre Marage*

Université Libre de Bruxelles, Boulevard du Triomphe, B-1050 Bruxelles, Belgium

*On behalf of the H1 and ZEUS Collaborations*

Recent results obtained at HERA on deeply virtual Compton scattering and exclusive vector meson production are reviewed, with the emphasis on the transition from soft to hard diffraction and on spin dynamics.

## 1 Introduction

Since the beginning of HERA data taking, a large number of studies have been performed of deeply virtual Compton scattering (DVCS) and of vector meson (VM) production. The exclusive final states include real photons [1, 2, 3], light ( $\rho$  [4, 5, 6, 7, 8, 9],  $\omega$  [10, 11] and  $\phi$  [12, 13, 7]) and heavy VMs ( $J/\psi$  [14, 15, 16, 17, 18],  $\psi(2s)$  [19] and  $\Upsilon$  [20, 21]). Cross sections are expressed in terms of  $\gamma^*p$  scattering.

In the presence of a hard scale, these processes provide unique information on the mechanisms of diffraction, in particular on the transition from soft to hard diffraction and on spin dynamics. A hard scale is provided by the VM mass  $M_V$ , by the negative square of the photon four-momentum,  $Q^2$  (with  $Q^2 \simeq 0$  for photoproduction and  $1.5 \leq Q^2 \leq 90 \text{ GeV}^2$  for electroproduction), or by the square of the four-momentum transfer at the proton vertex,  $t$ .

DVCS and VM production with small  $|t|$  values ( $|t| \leq 0.5 \text{ GeV}^2$  for elastic scattering and  $|t| \leq 2.5 \text{ GeV}^2$  for proton dissociation) are interpreted in terms of two complementary QCD approaches. Following a collinear factorisation theorem, the DVCS process, the electroproduction of light VMs by longitudinally polarised photons, and the production of heavy VMs can be described by the convolution of the hard process with generalised parton distributions in the proton (GPDs). High energy DVCS and VM production can also be described through the factorisation of virtual photon fluctuation into a  $q\bar{q}$  colour dipole, diffractive dipole–proton scattering, and  $q\bar{q}$  recombination into the final state photon or VM. The interaction scale  $\mu$  is given by the characteristic transverse size of the dipole, with  $\mu^2 \simeq (Q^2 + M_V^2)/4$  for light VM electroproduction by longitudinal photons and for heavy VM production, whereas this value may be significantly reduced for light VM electroproduction by transversely polarised photons, because of end-point contributions in the photon wave function. For DVCS, LO contributions are present, which suggests that the relevant scale may be  $Q^2$  rather than  $Q^2/4$  as for VMs.

Several models, based on either approach, have been proposed. They differ in particular in the way the VM wave function is taken into account, in the parameterisation of the parton distributions and of the dipole–proton scattering, and in the extension to non-zero  $|t|$  values of the scattering amplitude.

High  $|t|$  photoproduction, with  $2 \leq |t| \leq 30 \text{ GeV}^2$ , of real photons [3],  $\rho$  and  $\phi$  mesons [8, 9],

and  $J/\psi$  mesons [17, 18] offer specific testing grounds for the BFKL evolution.

Comparisons of models with the data are discussed in particular in [1, 2, 3, 6, 7, 9, 17, 18, 22].

## 2 Kinematic Dependences

**DVCS** The kinematic dependences of DVCS production, presented in Fig. 1, are well described by models using either GPDs or a dipole approach [1, 2].

The interference of the DVCS and Bethe-Heitler processes gives access, through the measurement of beam charge asymmetry, to the ratio  $\rho$  of the real to imaginary parts of the DVCS amplitude. The measurement  $\rho = 0.20 \pm 0.05 \pm 0.08$  [2] is in agreement with the value  $\rho = 0.25 \pm 0.03 \pm 0.05$  obtained from a dispersion relation using the  $W$  dependence of the cross section.

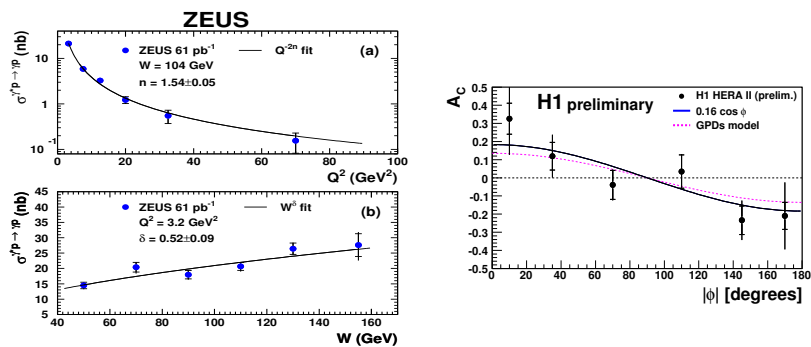


Figure 1: (left)  $Q^2$  and  $W$  dependences of DVCS production, with simple fit parameterisations [1]; (right) beam charge asymmetry,  $\cos \phi$  fit and predictions of a GPD model [2].

**$Q^2$  dependence of light VM production** The cross sections for elastic and proton dissociative  $\rho$  and  $\phi$  electroproduction have been measured with high precision [6, 7, 13]. The  $Q^2$  dependence, shown for  $\rho$  mesons in Fig. 2, is reasonably described by several models, using either the GPD or the dipole approach.

Although the production cross sections for light and heavy VMs differ by several orders of magnitude at  $Q^2 \simeq 0$ , it is striking that the ratios are nearly constant when they are studied as a function of the scaling variable  $(Q^2 + M_V^2)/4$ , with values close to unity when scaled according to the quark charge content of the VMs,  $\rho : \omega : \phi : J/\psi = 9 : 1 : 2 : 8$ . This confirms the relevance of the dipole size to the cross sections, even though the agreement with SU(4) universality is not perfect, indicating that wave function effects may need to be taken into account.

The ratio of the production cross sections with proton dissociative and elastic scattering at  $|t| = 0$  is found to be independent of  $Q^2$ . Consistent values around 0.160 are measured for  $\rho$  and  $\phi$  production with dissociative mass  $M_Y < 5$  GeV [7]. This observation supports the independence of the hard and soft vertex contributions to the scattering amplitudes, known as proton vertex or ‘‘Regge’’ factorisation.

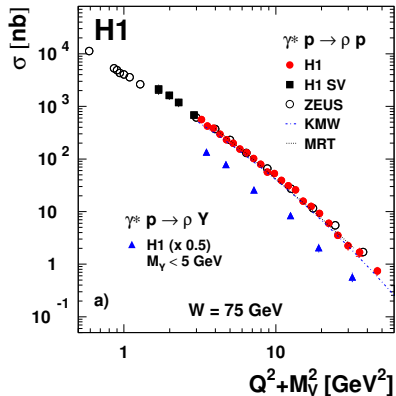


Figure 2:  $Q^2$  dependence of elastic and proton dissociative electroproduction cross sections of  $\rho$  mesons, and model predictions [7].

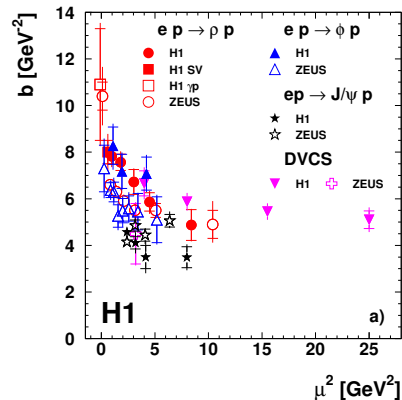


Figure 3: Elastic  $b$  slopes, as a function of  $\mu^2 = (Q^2 + M_V^2)/4$  for VM production and  $\mu^2 = Q^2$  for DVCS [7].

**$t$  slopes** Exponentially falling  $|t|$  distributions, with  $d\sigma/dt \propto e^{-b|t|}$ , are measured for DVCS, light and heavy VM production, in both the elastic and the proton dissociative channels. In an optical model approach, the slope  $b$  is given by the convolution of the transverse sizes of the  $q\bar{q}$  dipole, of the diffractively scattered system (which vanishes for proton dissociation) and of the exchange (a contribution which is expected to be small). As shown in Fig. 3, the elastic slopes for light VMs strongly decrease with increasing  $Q^2$ . They reach values of the order of  $5 \text{ GeV}^{-2}$ , similar to those measured in  $J/\psi$  production, for values of the scaling variable  $(Q^2 + M_V^2)/4 \gtrsim 5 \text{ GeV}^2$ . This evolution reflects the shrinkage with  $Q^2$  of the light quark colour dipole. A similar evolution is observed for DVCS as a function of the variable  $Q^2$ . The proton dissociative slopes similarly decrease with the increasing scale, down to values around  $1.5 \text{ GeV}^{-2}$  for  $\rho$  production and DVCS, and values slightly below  $1 \text{ GeV}^{-2}$  for  $J/\psi$  production.

The difference between the elastic and proton dissociative slopes,  $b_{el} - b_{p.diss.}$ , provides another test of proton vertex factorisation. A value of  $3.5 \pm 0.1 \text{ GeV}^{-2}$  is measured for  $J/\psi$  [14, 16], with a similar value for DVCS [2]. The difference is higher, around  $5.5 \text{ GeV}^{-2}$ , for  $\rho$  and  $\phi$  mesons, with however an indication of a decrease toward the  $J/\psi$  value with increasing  $(Q^2 + M_V^2)/4$  [7].

**Energy dependence and effective Regge trajectory** The energy dependence of DVCS and VM production is well described by a power law,  $d\sigma/dW \propto W^\delta$ .

Figure 4 (left) shows that the energy dependence is significantly stronger for heavy quark photoproduction, with  $\delta \sim 0.8 - 1.2$ , than for (soft) hadron-hadron interactions and light VM photoproduction, with  $\delta \sim 0.2$ . This is explained by the fact that the photoproduction of VMs formed of heavy quarks is a hard process, characterised by small transverse dipoles which probe the low- $x$  gluon density in the proton at a scale where it is quickly increasing with  $1/x$ .

For light VM production, the  $W$  dependence is hardening with  $Q^2$ , with values of  $\delta$  similar to the  $J/\psi$  values for  $(Q^2 + M_V^2)/4 \gtrsim 5 \text{ GeV}^2$ . This feature is explained by the shrinkage of the colour dipoles at large  $Q^2$  values.

In a Regge inspired parameterisation, the energy dependence of the cross section and its

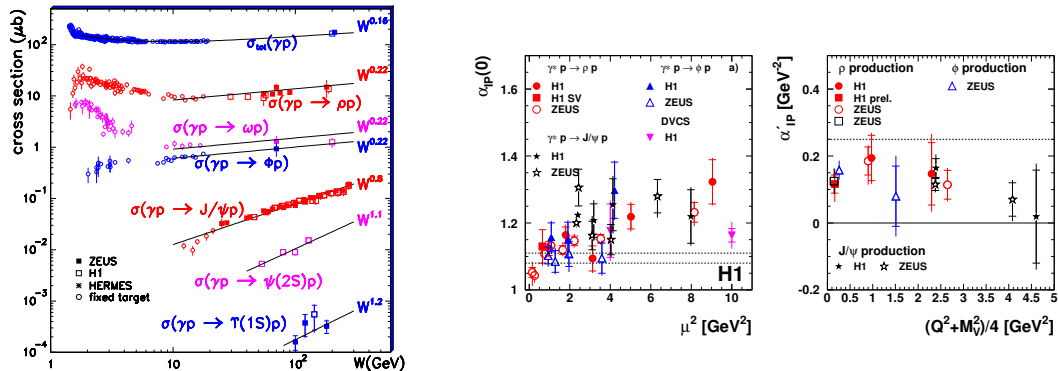


Figure 4: (left)  $W$  dependence of VM photoproduction [22]; measurement of the intercept  $\alpha_{\mathcal{P}}(0)$  (centre) and of the slope  $\alpha'$  (right) of the effective Regge trajectory, as a function of the scale  $\mu^2 = (Q^2 + M_V^2)/4$  for VM production and  $\mu^2 = Q^2$  for DVCS [7].

correlation with  $t$  are given by  $\delta(t) = 4(\alpha_{\mathcal{P}}(t) - 1)$ , with  $\alpha_{\mathcal{P}}(t) = \alpha_{\mathcal{P}}(0) + \alpha' \cdot t$ , where  $\alpha'$  describes the shrinking of the diffractive peak with energy. The hard behaviour of  $J/\psi$  production and the hardening with  $(Q^2 + M_V^2)/4$  of the energy dependence of light VM production for  $t = 0$  are shown in Fig. 4 (centre), where values of 1.08 or 1.11 for  $\alpha_{\mathcal{P}}(0)$  are typical of soft hadron-hadron interactions. As shown in Fig. 4 (right), the slope of the effective trajectory for VM production, including  $\rho$  photoproduction [5], is smaller than the value  $0.25 \text{ GeV}^{-2}$ , typical for hadronic interactions. For DVCS  $\alpha' = 0.03 \pm 0.09 \pm 0.11 \text{ GeV}^{-2}$  [2]; for  $J/\psi$  photoproduction at high  $|t|$ , combining H1 [17] and ZEUS [18] measurements,  $\alpha' = -0.02 \pm 0.01 \pm 0.01 \text{ GeV}^{-2}$ .

**Remarks on the interaction scales** The energy dependence of the total  $ep$  cross section at fixed values of  $Q^2$  can be parameterised as  $F_2 \propto x^{-\lambda}$ , with values of  $\lambda$  increasing with  $Q^2$ , a feature which is attributed to the increase with  $Q^2$  of the parton density at small  $x$ . The prediction that for VM production  $\delta = 2\lambda$ , when taken at the same scale, can thus provide information on the relevant effective scale for the reaction. The present results clearly indicate that the variable  $(Q^2 + M_V^2)/4$  is a better candidate than  $Q^2$  for such a unified scale, but high precision measurements of the energy dependence of  $\rho$  and  $J/\psi$  electroproduction remain necessary to settle the scale issue [22].

For the DVCS process, where both LO and NLO (dipole-type) diagrams contribute, the present high energy data seem to favour an effective scale  $\approx Q^2$  rather than  $\approx Q^2/4$  in order to ensure diffraction universality, but here also more precise data are required.

### 3 Spin Dynamics

The VM production and decay angular distributions allow the measurement of fifteen spin density matrix elements, which are bilinear combinations of helicity amplitudes. Under natural parity exchange, five  $T_{\lambda_V \lambda_\gamma}$  amplitudes are independent: two  $s$ -channel helicity conserving (SCHC) amplitudes ( $T_{00}$  and  $T_{11}$ ), two single helicity flip amplitudes ( $T_{01}$  and  $T_{10}$ ) and one double flip amplitude ( $T_{-11}$ ).

The  $Q^2$  dependence of the matrix elements for  $\rho$  and  $\phi$  production indicates that the five elements which contain products of the SCHC amplitudes are non-zero, whereas those formed with the helicity violating amplitudes are generally consistent with 0. A notable exception is the element  $r_{00}^5$ , which involves the product of the dominant  $T_{00}$  SCHC amplitude with  $T_{01}$ , which describes the transition from a transversely polarised photon to a longitudinal  $\rho$  meson [6, 7].

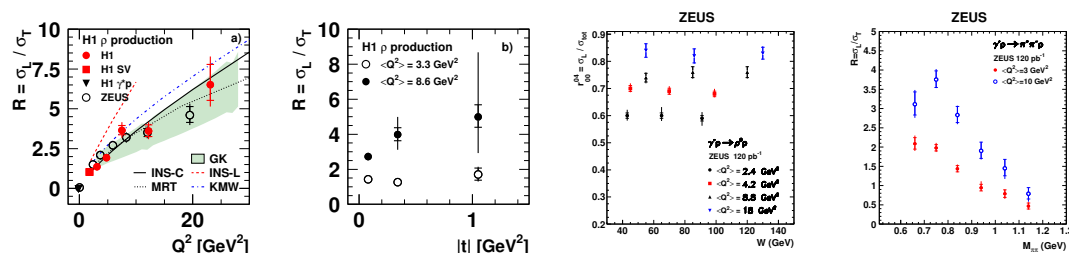


Figure 5: Measurement of  $R = \sigma_L/\sigma_T$ , as a function of  $Q^2$  and  $|t|$  [7],  $W$ , and the invariant mass,  $M_{\pi\pi}$ , of the two decay pions [6], for  $\rho$  electroproduction.

The ratio  $R = \sigma_L/\sigma_T$  of the longitudinal to transverse cross sections for  $\rho$  production is shown in Fig. 5 as a function of  $Q^2$ ,  $W$ ,  $t$ , and the invariant mass of the two decay pions, for several domains in  $Q^2$ .

A strong increase of  $R$  with  $Q^2$  is observed, which is tamed at large  $Q^2$ . These features are relatively well described by GPD and dipole models. The  $Q^2$  dependence of  $R$  for  $\rho$ ,  $\phi$  and  $J/\psi$  production follows a universal trend when plotted as a function of  $Q^2/M_V^2$  [7]. With the present data, no  $W$  dependence is observed, but it should be stressed that the lever arms in  $W$  for fixed  $Q^2$  values are relatively limited.

No  $|t|$  dependence is observed for  $R$  by ZEUS with  $|t| \leq 1 \text{ GeV}^2$  [6], whereas an increase of  $R$  with  $|t|$  is observed by H1 for  $Q^2 > 5 \text{ GeV}^2$ ,  $|t| \leq 3 \text{ GeV}^2$  [7]. This increase can be translated into a measurement of the difference between the longitudinal and transverse  $t$  slopes, through the relation  $R(t) = \sigma_L(t)/\sigma_T(t) \propto e^{-(b_L - b_T)|t|}$ . A slight indication ( $1.5\sigma$ ) is thus found for a negative value of  $b_L - b_T$  ( $-0.65 \pm 0.14_{-0.51}^{+0.41}$ ), suggesting that the average transverse size of dipoles for transverse amplitudes is larger than for longitudinal amplitudes.

The strong dependence of  $R$  with the dipion mass, observed by both experiments [6, 7], cannot be attributed solely to the interference of resonant  $\rho$  and non-resonant  $\pi\pi$  production, and indicates that the spin dynamics of  $\rho$  production depends of the effective  $q\bar{q}$  mass.

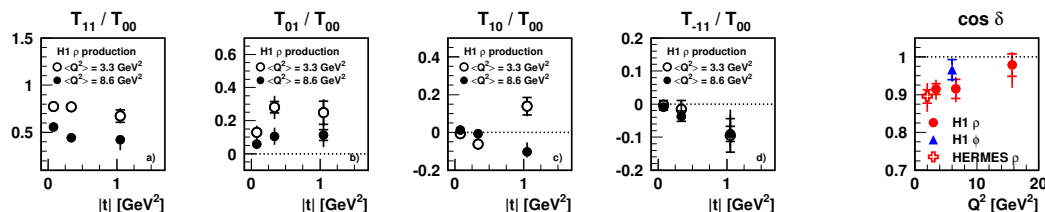


Figure 6: (a-d) Helicity amplitude ratios, as a function of  $t$ ; (right plot) phase difference between the two SCHC amplitudes,  $T_{00}$  and  $T_{11}$  [7].

Helicity amplitude ratios are measured, under the approximation that they are in phase, through fits to the 15 matrix elements. The four ratios to the dominant  $T_{00}$  amplitude are presented in Fig. 6 as a function of  $t$ , for two domains in  $Q^2$ . At large  $Q^2$ , a  $t$  dependence compatible with the expected  $\sqrt{|t|}$  law is observed for both single helicity flip amplitudes. A significant double-flip amplitude  $T_{-11}$  is observed, which may be related to gluon polarisation in the proton. The  $t$  dependence of  $T_{11}/T_{00}$  at large  $Q^2$ , a  $3\sigma$  effect, is related to the  $t$  dependence of  $R$  and supports the indication of a difference between the transverse sizes of dipoles in transversely and longitudinally polarised photons.

A small non-zero phase difference between the two SCHC amplitudes, which decreases with increasing  $Q^2$ , is visible in Fig. 6. Through dispersion relations, this non-zero value is suggestive of different  $W$  dependences of the longitudinal and transverse amplitudes.

## 4 Large $|t|$ VM Production

In exclusive real photon and VM production at high energy and large  $|t|$ , a hard scale is present at both ends of the gluon ladder which extends over a large rapidity range, between the struck parton in the proton (mostly gluons at small  $x$ ) and the quark or antiquark from the photon fluctuation. These processes thus offer a unique testing ground for the BFKL evolution, since no strong  $k_T$  ordering along the ladder is expected. This is at variance with high  $Q^2$  VM production at low  $|t|$ , where a large scale is present at the photon end of the ladder and a small scale at the proton end, a configuration which is described by the DGLAP evolution. For real photon and  $J/\psi$  production, there is little uncertainty related to the wave functions.

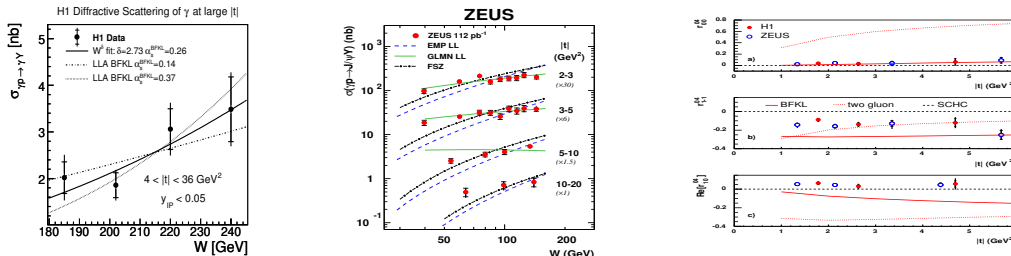


Figure 7: Large  $|t|$  photoproduction measurements:  $W$  dependence of real photon [3] (left) and  $J/\psi$  [18] production (centre); spin density matrix elements for  $\rho$  production [9].

A specific QCD prediction for large  $|t|$  production is the power-law dependence of the  $|t|$  distribution, at variance with the exponential dependence for  $|t| \lesssim$  a few GeV $^2$ . The  $t$  dependences for  $|t| \geq 4$  GeV $^2$  of  $\gamma$  and  $J/\psi$  production are indeed well described by power laws with exponents  $n = 2.60 \pm 0.19^{+0.03}_{-0.08}$  [3], and  $n = 3.0 \pm 0.1$  [18], respectively.

Figures 7 (left) and (centre) present the  $W$  evolutions of high  $|t|$  real photon and  $J/\psi$  production, respectively. A strong  $W$  dependence is observed, compatible with calculations based on the BFKL approach, whereas the DGLAP evolution (valid for  $|t| \leq m_\psi^2$ ), predicts a significantly weaker dependence.

The spin density matrix elements for  $J/\psi$  production are in agreement with SCHC [17, 18], whereas substantial helicity flip contributions are observed in Fig. 7 (right) for  $\rho$  production

with  $1.5 \lesssim |t| \lesssim 10 \text{ GeV}^2$  [8, 9], which can be understood in a BFKL approach with a chiral-odd component of the photon wave function.

## Acknowledgements

It is a pleasure to thank numerous colleagues from the ZEUS and H1 collaborations as well as theorists for enlightening discussions, and the workshop organisers for the lively discussions and the pleasant atmosphere of the meeting.

## References

- [1] S. Chekanov *et al.* [ZEUS Collab.], Phys. Lett. **B573** 46 (2003) [hep-ex/0305028]; *idem*, JHEP 0905 108 (2009) [arXiv:0812.2517].
- [2] F.D. Aaron *et al.*, [H1 Collab.], Phys. Lett. **B659** 796 (2008) [arXiv:0709.4114]; *idem*, *Deeply Virtual Compton Scattering and related Beam Charge Asymmetry in ep Collisions at HERA*, DESY-09-109 (2009) [arXiv:0907.5289].
- [3] F.D. Aaron *et al.* [H1 Collab.], Phys. Lett. **B672** 219 (2009) [arXiv:0810.3096].
- [4] J. Breitweg *et al.* [ZEUS Collab.], Eur. Phys. J. **C14** 213 (2000) [hep-ex/9910038]; *idem*, Eur. Phys. J. **C2** 247 (1998) [hep-ex/9712020]; M. Derrick *et al.* [ZEUS Collab.], Z. Phys. **C73** 253 (1997).
- [5] S. Aid *et al.* [H1 Collab.], Nucl. Phys. **B463** 3 (1996) [hep-ex/9601004]; B. List [H1 Collab.], *Extraction of the Pomeron Trajectory from a Global Fit to Exclusive  $\rho^0$  Meson Photoproduction Data*, Proc. of the XVII Int. Workshop on DIS and Related Subjects (DIS 2009), Madrid (2009) [arXiv:0906.4945].
- [6] S. Chekanov *et al.* [ZEUS Collab.], PMC Phys. **A1** 6 (2007) [hep-ex/0708.1478].
- [7] F.D. Aaron *et al.* [H1 Collab.], *Diffractive electroproduction of  $\rho$  and  $\phi$  mesons*, DESY-09-093 (2009).
- [8] S. Chekanov *et al.* [ZEUS Collab.], Eur. Phys. J. **C26** 389 (2003) [hep-ex/0205081].
- [9] A. Aktas *et al.* [H1 Collab.], Phys. Lett. **B638** 422 (2006) [hep-ex/0603038].
- [10] M. Derrick *et al.* [ZEUS Collab.], Z. Phys. **C73** 73 (1996) [hep-ex/9608010].
- [11] J. Breitweg *et al.* [ZEUS Collab.], Phys. Lett. **B487** 273 (2000) [hep-ex/0006013].
- [12] M. Derrick *et al.* [ZEUS Collab.], Phys. Lett. **B377** 259 (1996) [hep-ex/9601009].
- [13] S. Chekanov *et al.* [ZEUS Collab.], Nucl. Phys. **B718** 3 (2005) [hep-ex/0504010].
- [14] S. Chekanov *et al.* [ZEUS Collab.], Eur. Phys. J. **C24** 345 (2002) [hep-ex/0201043].
- [15] S. Chekanov *et al.* [ZEUS Collab.], Nucl. Phys. **B695** 3 (2004) [hep-ex/0404008].
- [16] A. Aktas *et al.* [H1 Collab.], Eur. Phys. J. **C46** 585 (2006) [hep-ex/0510016].
- [17] A. Aktas *et al.* [H1 Collab.], Phys. Lett. **B568** 205 (2003) [hep-ex/0306013].
- [18] [ZEUS Collab.], *Diffractive photoproduction of  $J/\psi$  mesons with large momentum transfer at HERA*, DESY-09-137 (2009).
- [19] C. Adloff *et al.* [H1 Collab.], Phys. Lett. **B541** 251 (2002) [hep-ex/0205107].
- [20] C. Adloff *et al.* [H1 Collab.], Phys. Lett. **B483** 23 (2000) [hep-ex/0003020].
- [21] S. Chekanov *et al.* [ZEUS Collab.], Phys. Lett. **B680** 4 (2009); doi:10.1016/j.physletb.2009.07.066.
- [22] A. Levy [ZEUS Collab.], *Electroproduction of vector mesons*, Proc. of the XVII Int. Workshop on DIS and Related Subjects (DIS 2009), Madrid (2009) [arXiv:0907.2178].